High Switching Ratio Variable-Temperature Solid-State Thermal Switch Based on Thermoelectric Effects.

Michael J. Adams[1], Mark Verosky[1], Mona Zebarjadi[2,3,*], Joseph P. Heremans[1,4,5,*]

1. Department of Mechanical and Aerospace Engineering, The Ohio State University, Columbus, Ohio

2. Department of Electrical and Computer Engineering, University of Virginia

3. Department of Materials Science and Engineering, University of Virginia

4. Department of Physics, The Ohio State University, Columbus, Ohio

5. Department of Materials Science and Engineering, The Ohio State University, Columbus, Ohio

* Address correspondence to m.zebarjadi@virginia.edu or heremans.1@osu.edu

Abstract

The switching ratio, the ratio between the thermal conductance in its off and on states, of a thermal switch is a critical design parameter of such a device. Here, we propose Peltier modules as a type of all-solid-state thermal switch that can operate over a wide temperature range and with an adjustable switching ratio. Calculations show that the switching ratio depends only on thermoelectric figure of merit and temperature bounds. A Peltier couple is constructed from Bi_2Te_3-based material and characterized by its thermal conductance and response time in the open condition and under an optimal activation current. The switching ratio diverges at small temperature differences with record-high measured values, an order of magnitude larger than achieved by other solid-state devices near room temperature. Materials with a high figure of merit could produce even larger switching ratios over higher temperature differences.

Keywords

Heat Switch; Solid-State; Peltier effect; Switching Ratio; Variable thermal conductance; Large temperature range; Time Constant

1. Introduction

A thermal switch acts as an on-off device for heat flux between a hot reservoir and cold reservoir by varying its own thermal conductance from K_{off} when the switch is open to a higher value K_{on} when the switch is closed (Figure 1a). Recently, thermal switches have become of great technological interest in heat management problems [1] because, unlike most thermal insulating of conducting layers that follow Fourier's law, they act as an active thermal circuit element. Applications scale from temperature regulation in cryogenic devices to regulating thermal storage for power generation. Active thermal circuits also make it possible to use temperature transients to increase the thermal efficiency of heat engines [1]. There are several technologies considered for thermal switches. Some rely on phase changes to regulate temperature under a heat load: superconducting or magnetic phase changes at liquid helium temperature [2] or crystalline phase change [3]. Passive switches based on phase change generally have switching ratios less than 5 [4], and each material works only in a narrow temperature range. Other designs are based on the electrical magnetoresistance of metal multilayers, which translate into a thermal magnetoresistance via the Wiedemann-Franz law. These have switching ratios limited by phonon conductivity, which acts as a thermal short, or require large applied magnetic fields [5]. A third type of thermal switch uses a gap filled by a thermally conducting fluid, e.g. a gas [6]. Similar active switches are MEMS thermal radiators and wetted nanoribbons [4], but all of these require mechanical activation or maintenance of vacuum. There is a need for thermal switches that operate entirely in the solid-state, work over a broad temperature range, and have a high thermal switching ratio.

Peltier modules are used commercially for refrigeration, pumping heat opposite to the natural direction. In that application, efficiency is limited by the materials' figure of merit zT

$$zT = \frac{\alpha^2 \sigma}{\kappa} T \tag{1}$$

where α, σ, and κ are thermopower, electrical, and thermal conductivity, respectively, for a given temperature T. Heat pumping also can be defined by the Peltier coefficient, which relates to thermopower via the Kelvin relation ?? = ????. When alternating n and p-type materials are combined in a device, we distinguish the materials' zT from the device's effective figure of merit ZT, which is further limited. We show here that the same modules can modulate the heat flux from a hot source to a cold source following an electrical input. In this configuration, one can view the Peltier module as an active thermal switch that opens and closes under an activation current (see Figure 1b). Consider a thermoelectric module placed between a hot source and a cold sink. The module acts as an open switch when there is no applied electric current, as shown in Figure 1c. In this case, the heat rate from the hot source to the cold source is merely passive heat conduction and could be expressed as:

$$Q_{off} = \kappa A (T_H - T_C)/L \tag{2}$$

where ?? is the cross section, L is the length of a given thermoelectric leg, $??_{??}$ is the hot source temperature, and $??_{??}$ is the cold side temperature. The thermal conductance of the switch in off position is $K_{off} = \kappa A/L$. The module acts as a closed switch when driving an electric current through the legs, shown in Figure 1d, with operating characteristics shown in Figure 1b. The heat rate under electrical input has two additional components: first is the Peltier current, which is proportional to electrical current with the Peltier coefficient, and second is the back-heat flux, which is the result of Joule heat generated within the thermoelectric legs. Upon solving the heat conduction equation and using constant temperature boundary conditions at the hot side and cold side, it can be shown that exactly half of the generated Joule heat returns to each end of the leg [7]. The heat rate at the hot side of the closed switch combines these terms:

$$Q_{on} = \kappa A(T_H - T_C)/L + \alpha T_H I - RI^2/2 \qquad \text{(3a)}$$

where the first term is the heat conduction rate, the second term is the Peltier current, and the third term is the back flow of Joule heating at hot side, where ?? is the resistance and ?? is the applied current. The switching ratio is then ??????/????????, which can be tuned from 1 to a maximum value dependent on the applied current. The maximum switching ratio then depends on the maximum ?????? with respect to current:

$$Q_{on-max} = \kappa A(T_H - T_C)/L + (\alpha T_H)^2/2R \quad \text{(3b).}$$

Therefore, the maximum switching ratio is:

$$\eta = Q_{on-max}/Q_{off} = 1 + (zT_H)\, T_H/(2\Delta T) \text{ (4a).}$$

Since we performed the calculations under constant temperature boundary conditions, note that the switching ratio reported in Eq 4a is the same as the ratio of effective thermal conductance, K = ????/??, in on and off modes. With constant device size, it is also equal to the ratio of effective thermal conductivity

$$\eta = K_{on-max}/K_{off} = \kappa_{on-max}/\kappa_{off} \qquad \text{(4b).}$$

Under these conditions, the ratio of the heat rejected to the cold side in the on and off mode is

$$\frac{Q_{c-on}}{Q_{off}} = 1 + \frac{ZT_H}{\Delta T}\left(T_c + \frac{1}{2}T_H\right) \qquad \text{(5).}$$

Clearly, as the heat flux extracted from the hot side increases, the heat rejected to the cold side (Q_C) increases even further. Therefore, the cold side should be connected to a high-capacity heat reservoir. For some applications, such as magneto-caloric refrigeration, Peltier modules are proposed to switch from off mode to refrigeration cycle mode [8]. In that case, it is desirable to maximize the ratio of the heat pumped from cold to hot in the "on" mode to the heat leaks from the hot side to the cold side in the "off" mode. Since the two heat fluxes are in the opposite directions, it means we should optimize $\frac{-Q_{C-on-max}}{Qoff}$. Using the same approach as before, the optimum ratio can be written as

$$\frac{-Q_{C-on-max}}{Qoff} = \frac{1}{2}\frac{ZT_c{}^2}{\Delta T} - 1 \qquad \text{(6).}$$

The results for a thermoelectric module with many n-p legs electrically in series and thermally in parallel is the same as Eq 4a wherein the material zT is replaced with the device ZT. Notice that the switching ratio is only a function of ZT and temperature boundaries. For example, with T_H of 400 K, ΔT of 40 K, and ZT of 1, the switching ratio is 6. This means if the thermal conductance of the module is 1 (W/K), it is possible to increase it to 6 (W/K), whereas if the thermal conductance is 10 (W/K), then it is possible to increase it to 60 (W/K).

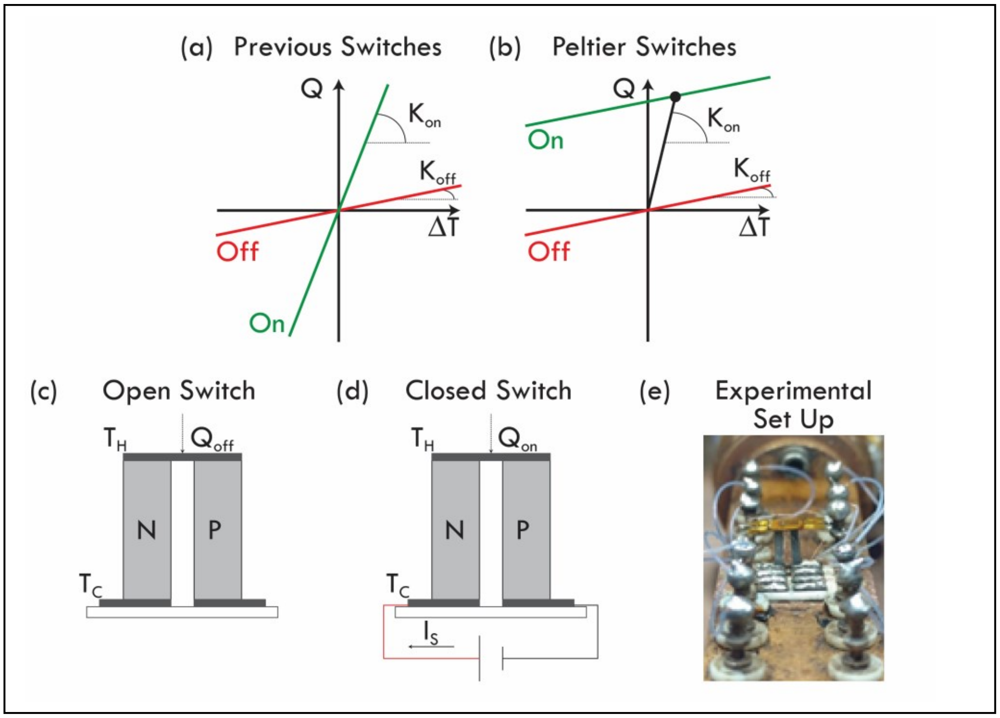

Figure 1. Schematic diagrams of a Peltier couple used as thermal switch. **(a)** Operating characteristics of a conventional heat switch. The slope of the $Q/\Delta T$ curves are the thermal conductances K_{on} and K_{off}; **(b)** Operating characteristics of a Peltier heat switch, where $K_{on} = Q_{on} / \Delta T$ depends on the operating point and is given by Eq. (3a); **(c)** Open switch: the passive thermal conductance alone determines the heat flow Q; **(d)** Closed switch: passive conductance and Peltier heat flow combine to give Q_{on} and the conductance K_{on}; and **(e)** Experimental measurement setup.

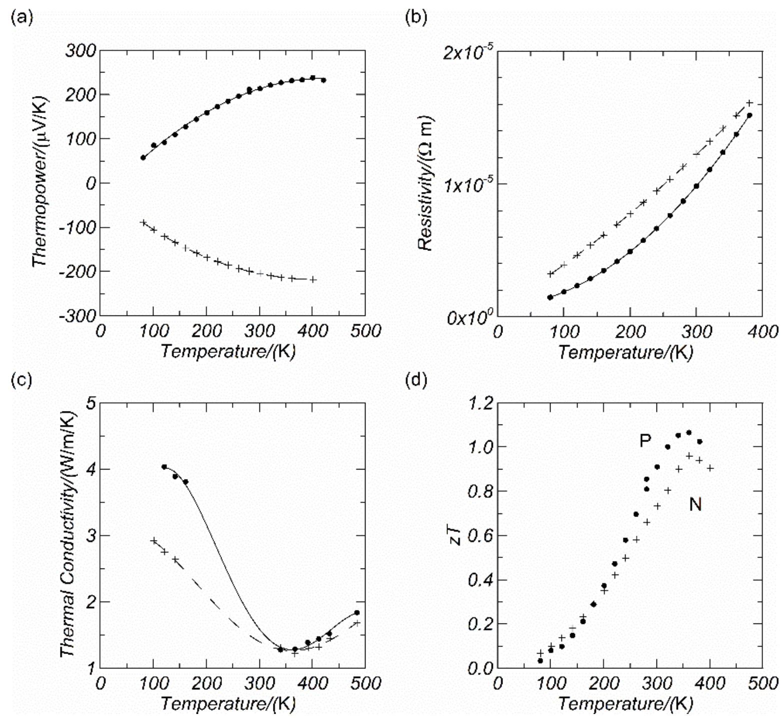

Figure 2. Properties of the n and p-type thermoelectric materials used to build the thermal switch **(a)** Thermopower **(b)** Resistivity **(c)** Thermal conductivity **(d)** Material *zT*. The lines are guides to the eye.

2. Materials and Methods

The Peltier couple was constructed from commercial Bi_2Te_3-based materials [9] used in Peltier modules. The p-type material is Sb-rich $(Sb,Bi)_2Te_3$ with a Hall carrier concentration of 2 to 2.5 x 10^{19} cm^{-3}. The n-type material is mostly Bi_2Te_3 with a Hall carrier concentration of 2.5 to 3 x 10^{19} cm^{-3}. Figure 2 shows the thermoelectric transport properties of the p-type and n-type legs, represented by circles and plus signs respectively. Thermopower, resistivity, and thermal conductivity were measured from 80 to 400 K. These follow similar trends with temperature for both materials, with a material *zT* near 1 above room temperature.

The legs were soldered to copper strips for current flow and seated on an alumina base. The base of the device was attached to a cryostat, which acted as a heat sink. A resistive heater attached to the top of the couple generated heating loads, while the temperature gradient T_H-T_C was measured by a copper-constantan thermocouple, which was isolated electrically from the device. The first experiment determined the optimal electric current for heat pumping. With no generated heat load, the module performed as a refrigerator, and optimal electrical input produced the maximum temperature difference. The data from Peltier cooling are shown in Figure 3. Device *ZT* is proportional directly to maximum temperature difference and inversely to the absolute cold side temperature.

$$ZT = 2\Delta T_{max}/T_C \qquad (7)$$

The values of ΔT_{max} were read from the plots of ΔT vs I_S in Figure 3a, and converted into a value of ZT via equation (7); they are then plotted in Figure 3b. As can be seen, the device ZT is only about half the average material zT, indicating that the electrical and thermal contact resistances in our device were not optimized.

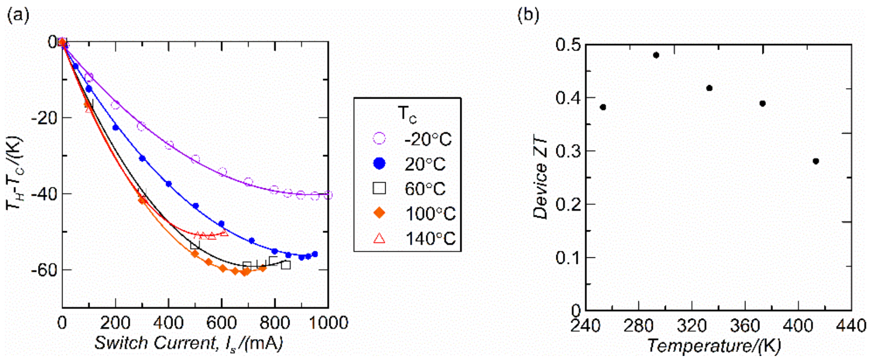

Figure 3. (a) Device in Peltier cooling mode: temperature drop as a function of Peltier drive current (the lines are guides to the eye) **(b)** Device ZT obtained from Peltier cooling measurements in (a)

Next, a heat load was generated at the top of the couple, so that it performed as a switch. The temperature difference was measured in the open (zero I_s) and closed (optimal I_s) modes with varying heater power, which is the product of current driven and voltage applied to the resistive heating element. Data from the switch experiment are shown in Figure 4. Finally, a timed switching experiment was performed. With a constant heat load, the device was switched on/off and the normalized change of the ΔT response recorded.

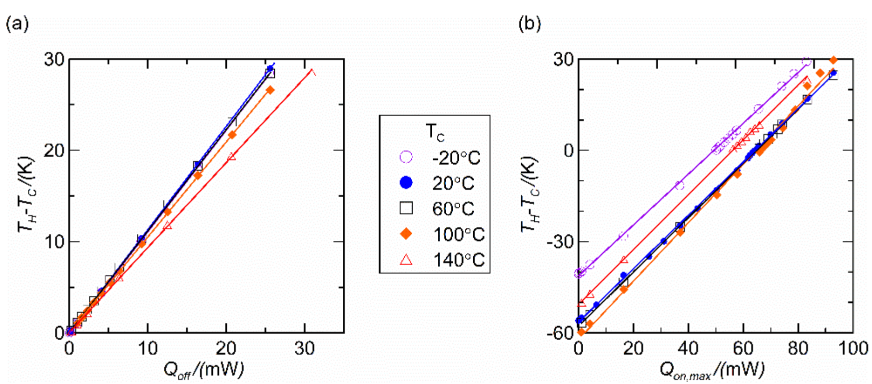

Figure 4. Temperature difference versus heat flow at the various background temperatures notes in the legend; **(a)** open switch in passive mode; **(b)** closed switch operating with the current I_s that maximized the ΔT in Figure 3a.

3. Results and Discussion

3.1 Switching Ratio

Linear trend lines were fitted to the switching data in Figure 4. These are used to calculate effective thermal conductance in each mode, which is equal to the ratio of heater power and temperature difference:

$$K_{off} = Q_{off}/\Delta T \tag{8}$$

$$K_{on-max} = Q_{on-max}/\Delta T \tag{9}$$

The ratio *K????-??????/K??????* defines the measured switching ratio. Figure 5 compares the measured switching ratio with the theoretical switching ratio, which is calculated using Eq 4a using measured device *ZT* reported in Figure 3b. The two curves are in good agreement with deviations less than 12% in the entire range. Measured switching ratios at small temperature differences are over 100. Contributions to deviation could include radiative heat losses and changes in effective *ZT* with increasing temperature gradient. Deviation is smallest at temperatures where the material *zT* is turning over (i.e., more level) and larger where *zT* is changing sharply.

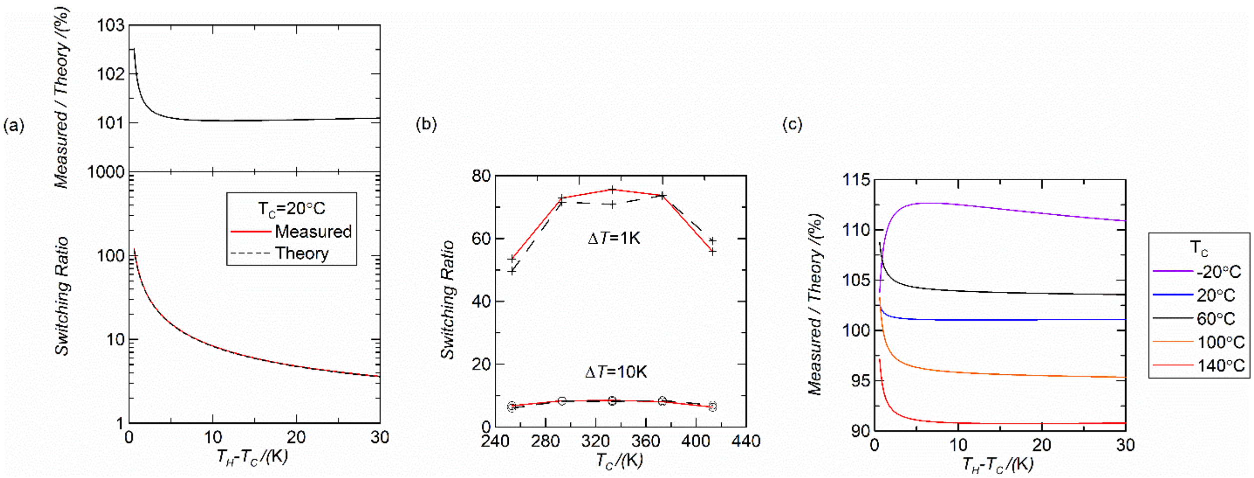

Figure 5. (a) Switching Ratio (bottom frame) and deviation between theory and observation (top frame) at 20 °C **(b)** Switching Ratio vs T_C. Red lines represent measured values and black dashed lines are theory. **(c)** Ratio between the measured and theoretical switching ratios for all temperatures.

3.2 Timed Response

The timed response at 20 °C is shown in Figure 6. The time constant of the exponential decay was found by normalizing the data and fitting an exponential function. At each temperature, the time constant was approximately 11.1 s with exception of 11 s at 140 °C. The time constant can be estimated using the formula ?? = $R_{th}C_{th}$. The device thermal resistance, R_{th} = 1100 (K/W), is measured from the thermal conductance of the device under open circuit conditions. The heat capacity C_{th} is the sum of the heat capacities of the n-type leg, the p-type leg, and the heater assembly, each calculated from their weight and published values of the specific heat of their constituents. The time constant ?? is finally calculated to be 11.6 s which is very close to the measured value.

Thus, we identify the origin of the response time as due to the heat diffusion equation in the couple. This enables detailed engineering analysis to be made for each application. In particular, the response time must be proportional to the square of length of the thermoelectric legs and decrease significantly when shorter legs are used. The contact resistance losses are relatively more important in Peltier couples with shorter elements. They will decrease the device *ZT* and, thus, both its power efficiency and the switching ratio (see equation 4). Therefore, the design of any given heat switch can trade off switching ratio for response time.

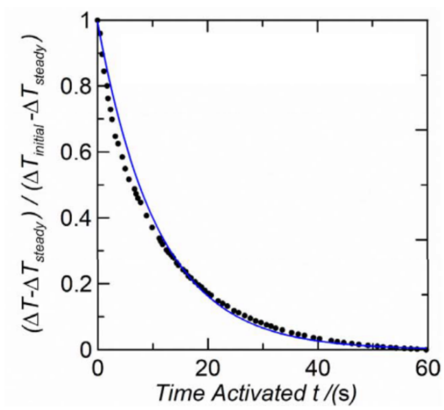

Figure 6. Time dependence of the normalized response at 20 °C. The data points are the dots. The fit to a function exp(-t/τ) with τ=11.1 s is the blue line.

4. Conclusions

We propose a new operating mode for Peltier couples as thermal switches. They offer a variable switching ratio, which can reach 100 for small temperature differences. When made from Bi_2Te_3-based material, they offer a nearly temperature-independent performance from -20 to 140 °C. The response time of the prototype couple made here is 12 seconds, but, since it is limited by the thermal diffusion length, it could be made shorter with shorter devices: an optimum between response time, drive current, and switching ratio can be engineered. The device model reproduces the results very well: as predicted by the theory, the switching ratio diverges with large values at small ΔT. *ZT* and response time can be improved by optimizing the shape of the module. Bi_2Te_3-based materials perform best near room temperature, but this approach can be applied to a larger range with other thermoelectric materials. At cryogenic temperatures, BiSb alloys have the largest *zT*, which would give the best switching ratio. On the other hand, metals with high thermopower such as $CePd_3$ [10] or Cobalt [11] could pump much larger heat fluxes at the expense of a higher leak rate in the open mode. Finally, most other solid-state coolers [12] also could work for the purpose of switching thermal conduction.

Acknowledgement

M.J.A. and J.P.H. are supported by the Ford-OSU alliance 2017 program. Work at UVA is supported by NSF Career award [grant number 1653268].

References

[1] G. Wehmeyer, T. Yabuki, C. Monachon, J. Wu, and C. Dames, Appl. Phys. Rev. **4**, 41304 (2017).

[2] W. Reese and W.A. Steyert, Rev. Sci. Instrum. **33**, 43 (1962).

[3] E. Sunada, K. Lankford, M. Pauken, K.S. Novak, and G. Birur, in *AIP Conf. Proc.* (AIP, 2002), pp. 211–213.

[4] K. Kim and M. Kaviany, Phys. Rev. B **94**, 155203 (2016).

[5] J.M.L. Engels, F.W. Gorter, and A.R. Miedema, Cryogenics (Guildf). **12**, 141 (1972).

[6] R.P. Bywaters and R.A. Griffin, Cryogenics (Guildf). **13**, 344 (1973).

[7] T.L. Bergman, A.S. Lavine, F.P. Incropera, and D.P. DeWitt, *Introduction to Heat Transfer*, 6th ed. (John Wiley and Sons, Inc., Hoboken,NJ, 2011).

[8] Tomc, U., Tušek, J., Kitanovski, A., & Poredoš, A., A new magnetocaloric refrigeration principle with solid-state thermoelectric thermal diodes. Applied Thermal Engineering, 58(1-2), 1-10 (2013).

[9] J.P. Heremans, R.J. Cava, and N. Samarth, Nat. Rev. Mater. **2**, 17049 (2017).

[10] S.R. Boona and D.T. Morelli, Appl. Phys. Lett. **101**, 101909 (2012).

[11] S.J. Watzman, R.A. Duine, Y. Tserkovnyak, S.R. Boona, H. Jin, A. Prakash, Y. Zheng, and J.P. Heremans, Phys. Rev. B **94**, 144407 (2016).

[12] A. Ziabari, M. Zebarjadi, D. Vashaee, and A. Shakouri, Reports Prog. Phys. **79**, (2016).